

# SCIENTIFIC REPORTS

**OPEN**

## Electron beam detection of a Nanotube Scanning Force Microscope

Alessandro Siria &amp; Antoine Niguès

Atomic Force Microscopy (AFM) allows to probe matter at atomic scale by measuring the perturbation of a nanomechanical oscillator induced by near-field interaction forces. The quest to improve sensitivity and resolution of AFM forced the introduction of a new class of resonators with dimensions at the nanometer scale. In this context, nanotubes are the ultimate mechanical oscillators because of their one dimensional nature, small mass and almost perfect crystallinity. Coupled to the possibility of functionalisation, these properties make them the perfect candidates as ultra sensitive, on-demand force sensors. However their dimensions make the measurement of the mechanical properties a challenging task in particular when working in cavity free geometry at ambient temperature. By using a focused electron beam, we show that the mechanical response of nanotubes can be quantitatively measured while approaching to a surface sample. By coupling electron beam detection of individual nanotubes with a custom AFM we image the surface topography of a sample by continuously measuring the mechanical properties of the nanoresonators. The combination of very small size and mass together with the high resolution of the electron beam detection method offers unprecedented opportunities for the development of a new class of nanotube-based scanning force microscopy.

Nanoscience and nanotechnology rely on the ability to manipulate and probe objects with a resolution in the deep nanometer range<sup>1-4</sup>. In the last three decades, advances in the field have been possible mainly thanks to the development of Atomic Force Microscopy (AFM)<sup>5-7</sup>. The idea behind the technique is at the same time very simple to understand and impressive in the attainable results: a tiny mechanical oscillator with a sharp tip at the extremity is approached to a surface and the evolution of the mechanical properties of the probe is monitored to get information about the sample topography and properties. Generally the mechanical oscillator used in AFM is a micrometer sized silicon cantilever presenting a very sharp tip at the extremity<sup>8</sup>. The need to increase the force sensitivity and spatial resolution, pushed the researchers to develop alternative mechanical oscillators based on self-assembled structures with submicrometer dimensions. Prominent examples are silicon based nanowires<sup>9, 10</sup> and carbon or boron nitride nanotubes<sup>11-14</sup> and even bidimensional suspended membranes<sup>15, 16</sup>. These new probes, because of their minute size and mass and almost perfect crystallinity, couple high spatial resolution and force sensitivity reaching the zepto-newton ( $10^{-24}$  N) range<sup>17</sup> for carbon nanotubes working in cryogenic environment. The major drawback for the further development of this new kind of probes is the extreme difficulty to detect their position and motion. It is worth mentioning that the mechanical properties of suspended nanowires have been elegantly measured via optical interferometry<sup>18</sup> leading to a first proof of concept of nanowire based scanning force microscope<sup>19</sup>. Despite the effort and recent progress, optical detection schemes can be hardly applied to nanotubes which are the ultimate mechanical oscillators and force sensors: their diameter, in fact, ranging from 1 nm to few tens of nanometers, is too small to be possibly detected with optical techniques. Very recently, electron microscopy has been shown to detect the thermally induced resonant properties of nanomechanical resonators with picogram effective masses<sup>9</sup> and even attogram scale carbon nanotubes<sup>20</sup>.

In this study we demonstrate that electron beam detection of mechanical oscillators can be harnessed to develop the first example of scanning force microscope based on individual suspended nanotubes. The individual nanotube is mounted on top of a custom AFM working *in situ* in a Scanning Electron Microscope (SEM) at a pressure of  $\approx 10^{-5}$  mbar. The highly focused electron beam of the SEM is positioned, in the so-called “spot mode”,

Laboratoire de Physique Statistique, Ecole Normale Supérieure, UMR CNRS 8550, PSL Research University, 75005 Paris Cedex 05, Paris, France. Alessandro Siria and Antoine Niguès contributed equally to this work. Correspondence and requests for materials should be addressed to A.S. (email: [alessandro.siria@ens.fr](mailto:alessandro.siria@ens.fr)) or A.N. (email: [antoine.nigues@ens.fr](mailto:antoine.nigues@ens.fr))

on the externally driven nano-oscillator and the inelastically scattered electrons (SE) are monitored to measure the resonator motion with a spatial resolution of 0.4 nm. As in standard non-contact AFM, the mechanical response of the nanotube is monitored via amplitude and phase locking, while approaching a sample, allowing to reconstruct the surface topography. This new technique allows to take advantage of the exceptional properties of nanotubes as force sensors for scanning microscopy. For standard electron microscopy, the spatial resolution, given by the electron beam size, is below 1 nm and it represents a three orders of magnitude improvement with respect to optical techniques. The high focusing of the electron beam further increases the motion detection resolution for unidimensional systems<sup>9,20</sup>. We therefore demonstrate for the first time, that one dimensional oscillators can be used for scanning force microscopy.

In this work we used boron nitride multiwalled nanotubes (BNNTs) realized via Chemical Vapour Deposition (CVD)<sup>21</sup>. CVD BNNTs present a very high structural purity with no evident defects in a spatial region reaching the micrometric range. The nanotubes are glued at the extremity of an electrochemically etched tungsten tip, fixed on a three axis piezo inertial motor mounted inside a SEM (FEI-Nova nanoSEM). In Fig. 1 we present a scheme of the experimental set-up and a SEM picture of one nanotube used in this study in front of an electrochemically etched tungsten tip. The electron beam is set fixed at a chosen working point along the section of the NT. This working point is chosen so that the variation of the SE intensity around this working point stays linear, see Fig. 1e. To counteract the drift of the nanotube with respect to the electron beam, a feedback loop acts directly on the SEM deflection coils to control the position of the electron beam and keep constant the low frequency component of emitted secondary electron (SE) intensity detected via a Everhart-Thornley Detector (ETD). This allows to maintain, for the whole duration of the experiment, the electron beam at a constant working position. The intensity of the emitted SE are recorded via a Specs Nanonis SPM electronics and analyzed to extract the DC and AC fluctuating components.

BN nanotubes are mechanically excited with an external piezo dither and the variations of SE, related to the relative displacement of the NT around the working point, are recorded as a function of the excitation frequency. When excited by an external sinusoidal force  $F_{ext}(\omega) = F_{ext}e^{i\omega t}$ , the nanotube behaves in first approximation as a spring-mass system with oscillation amplitude and phase with respect to the excitation given by:

$$A(\omega) = \frac{F_{ext}}{\sqrt{m_{eff}^2(\omega_0^2 - \omega^2)^2 + \gamma^2\omega^2}} \quad (1)$$

$$\phi(\omega) = \arctan\left(\frac{\gamma\omega}{m_{eff}(\omega_0^2 - \omega^2)}\right) \quad (2)$$

with  $m_{eff}$  the oscillator effective mass,  $\omega_0 = \sqrt{\frac{k}{m_{eff}}}$  the resonant frequency and  $\gamma$  the damping factor.  $k$  is the spring constant that is for this nanotube in the order of  $\approx 10^{-4}$  N/m to compare to the typical spring constant for multi-walled carbon nanotube that is in the range of 0.001–0.05 N/m<sup>22</sup>. Using single wall nanotube, the value of the spring constant can be substantially pushed down to value of  $10^{-6}$ – $10^{-5}$  N/m. These values have to be compared to what generally achievable with standard Silicon cantilever that is at best in the order of few mN/m. However general dynamic mode cantilevers have spring constants in the range of few tens of N/m which give a force resolution 4 order of magnitude lower than what possible with individual nanotubes.

In Fig. 2a we present the response of a nanotube with diameter  $D \approx 50$  nm and length  $L = 18 \mu\text{m}$ , when varying the frequency of excitation. The mechanical response is characterised by a resonance at  $f_0 = \omega_0/2\pi \approx 270$  kHz and a quality factor, defining the inverse of the damping rate,  $Q \approx 250$ . In contrast to previous studies on nanowires and single walled carbon nanotubes<sup>9,19,20</sup>, we do not observe a double resonant peak due to non degeneracy of polarisations. This further confirms the high structural quality and geometrical symmetry of BN nanotubes used during this work.

To confirm that the detected resonance is due to the mechanical motion of the nanotube, we switch the SEM operation mode from “spot mode” to the conventional full frame imaging: when excited at the resonance the nanotube position exhibits the standard resonant profile for the fundamental mode of a single clamped oscillator, as described by the Euler-Bernoulli equation. In Fig. 2c we plot the SEM images for different excitation amplitudes confirming that for the range of excitations used during the experiment, the oscillator stays in its linear regime.

As the interaction of the oscillator with its environment is modified, one observes a change in both the frequency and the amplitude at resonance. The shift in resonance frequency  $\delta f$  is related to the conservative force response, whereas the broadening of the resonance (change of quality factor  $Q_0 \rightarrow Q_1$ ) is related to dissipation:<sup>23</sup>

$$\frac{\partial F_i}{\partial r_i} = 2k_i \frac{\delta f_i}{f_{0,i}} \text{ and } F_{D,i} = \frac{k_i}{\sqrt{3}} \left( \frac{1}{Q_0} - \frac{1}{Q_1} \right) \quad (3)$$

where the index  $i$ , indicates the component of the position vector. In practice, during a typical experiment, two feedback loops allow us to work at the resonance and maintain constant the oscillation amplitude  $a_0$ . Monitoring the frequency shift  $\delta f$  and the resonance quality factor  $Q_r$ , obtained from the excitation voltage or the oscillation amplitude, thus provides a direct measurement of real and imaginary parts of the mechanical impedance.

To demonstrate the possibility to use a nanotube as the force sensor of a scanning probe microscope, we firstly approached a very sharp tungsten tip to the oscillating nanotube. While approaching the tungsten tip down to

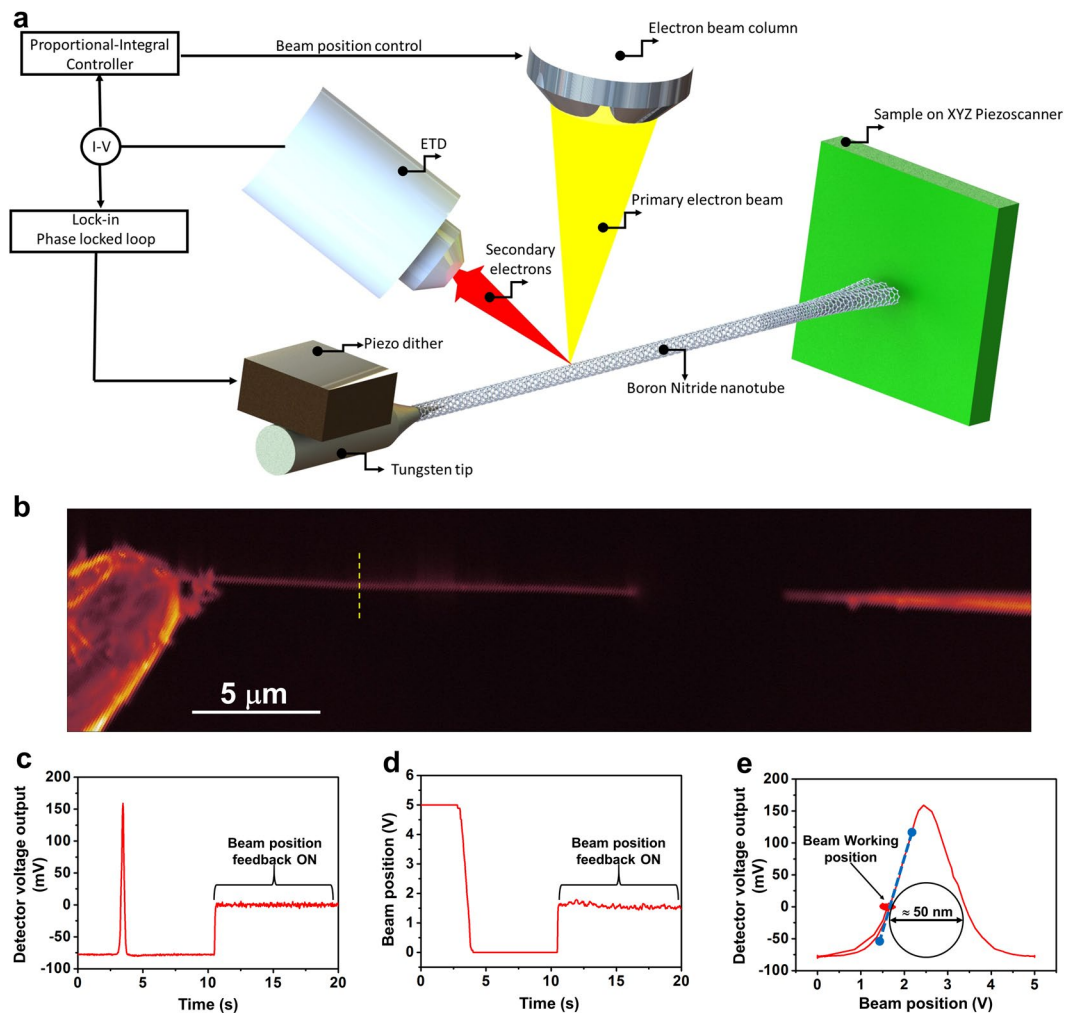


**Figure 1.** Experimental set-up. **(a)** Schematic drawing of the experimental set-up; a boron nitride nanotube on top of a custom AFM is excited at the resonant frequency by an external piezo dither. The secondary electrons emitted by the nanotube irradiated by an electron beam are recorded via an ETD detector. The DC component of the signal is used to fix the position of the electron beam with respect to the nanotube by acting on the electron beam deflection coils through a feedback loop; the AC intensity fluctuations record the mechanical motion of the oscillator. **(b)** Scanning Electron Microscope picture of one boron nitride nanotube used during the study; measured nanotube diameter  $D = 50 \text{ nm}$  and length  $L = 18 \text{ }\mu\text{m}$  in front of a tungsten tip. Yellow dashed line corresponds to the cross section presented in **(c)** and **(e)**. **(c)** Secondary electron intensity converted in voltage detected during a line scan over the nanotube; at  $t = 10 \text{ s}$  the feedback loop acting on the deflection coils is activated to keep the SE intensity at a defined set-point, 0 V here. **(d)** Voltage applied to the deflection coils to control the position of the electron beam; at  $t = 10 \text{ s}$  the feedback loop is activated to keep constant the low frequency component of SE intensity. **(e)** SE intensity **(b)** as a function of the voltage applied **(c)** to control the position of the electron beam; once the feedback loop is activated the working position (red sputtered) is attained and the intensity of the SE is fixed by changing the applied voltage to the deflection coils; the slope of the blue dashed line determines the amplitude calibration to be  $125 \text{ nm/V}$  for this position along the tube.

the contact we record the evolution of the phase between the nanotube oscillation and the exciting dither and of the oscillation amplitude. This first experiment is performed in an open-loop configuration: any variation of the interacting environment is directly measured by a change of both the oscillation amplitude and the phase with respect to the excitation. Once the mechanical response of the NT is modified by the tip-NT interaction, we kept the distance constant and we performed a scanning picture of the tungsten tip, as in standard AFM. As shown in Fig. 3a, the amplitude and phase shift as a function of the position of the tip correctly detect the spatial force field induced by the tungsten, and consequently reconstruct the tip shape.

As a further demonstration of the potentialities of the NT-SFM, a BNNT (diameter  $D = 80 \text{ nm}$  and length  $L = 20 \text{ }\mu\text{m}$ ) with resonant frequency  $f_0 \approx 350 \text{ kHz}$  and oscillation amplitude of  $\approx 10 \text{ nm}$  scans at a distance of  $\approx 10 \text{ nm}$  a (100) silicon surface while a double feedback loop acts on both the phase and the amplitude. In Fig. 3b we plot a cartography of a 1 micron silicon terrace, recording at the same time the excitation voltage applied to

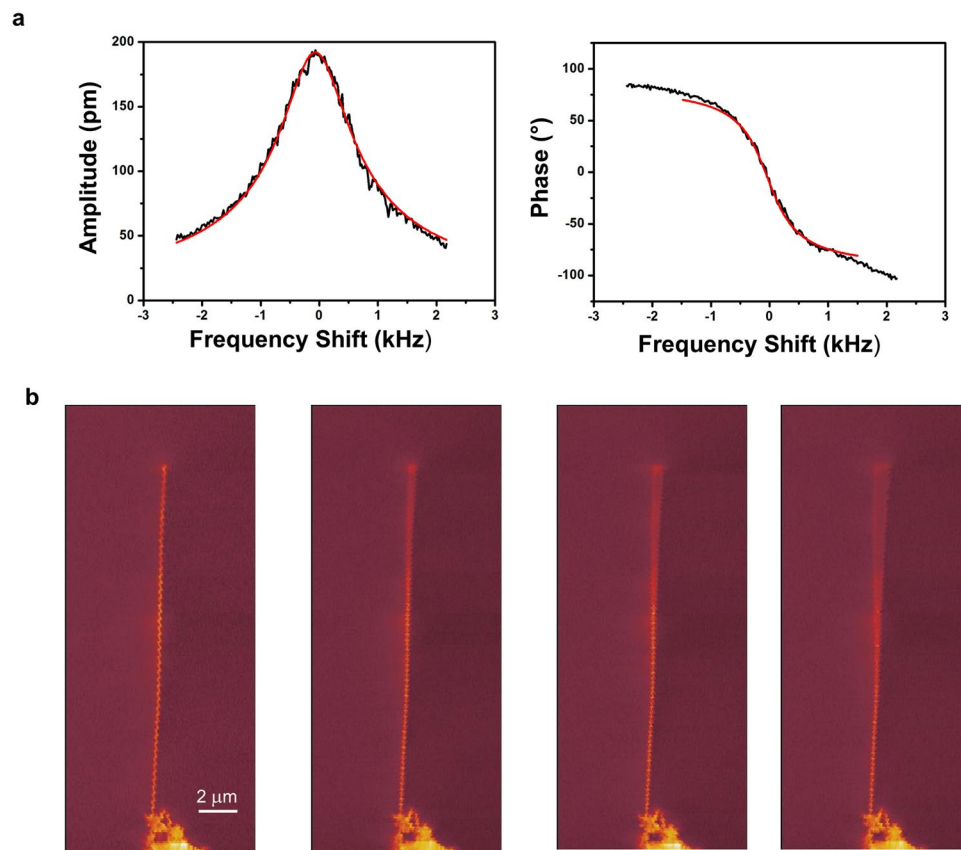


**Figure 2.** Electron beam detection of the mechanical response of a BN nanotube. **(a)** Amplitude and phase of the nanotube mechanical response as a function of the exciting frequency. The frequency is scanned around the resonant frequency; for a BN nanotube with  $D = 50$  nm and  $L = 18$   $\mu\text{m}$  the resonance is measured at  $f_0 = \omega_0/2\pi \approx 270$  kHz and the quality factor  $Q \approx 250$ . Red curves are best fit based on equations (1) and (2). **(b)** Scanning Electron Microscope pictures of the nanotube for different excitation amplitudes: from left to right 0 mV, 500 mV, 1 V, 2 V; the mode shape reproduces well the standard Euler-Bernoulli profile for the fundamental mode of a single clamped tube.

keep constant the amplitude and the frequency shift. Variations of both quantities allow to reconstruct the surface topography with a resolution of  $\approx 100$  nm, given by the size of the nanotube apex.

Finally taking benefit from the versatility of the NT-SFM and in addition to what presented above, we show in Fig. 3c, a static AFM and a SEM picture of gold nanoparticles deposited on a HOPG sample. In this case, by static we mean that the nanotube is neither excited nor oscillating; this operation mode is the analog of the static mode employed in standard Atomic Force Microscopy. The static AFM picture is obtained by recording the deflection of the nanotube during the scan; experimentally this quantity is given by the voltage command to the deflection coils to keep constant the SE emission intensity. When the nanotube deflects because of the interaction with the surface, its relative position with respect to the electron beam changes, therefore modifying the SE emission intensity. The feedback loop acting on the beam position allows to reconstruct precisely the displacement of the nanotube and consequently the surface topography.

In addition, it is worth mentioning the complementarity of this operation mode with the AC mode presented before: by recording the deflection of the nanotube it is in fact possible to quantitatively measure the total force which the nanotube is submitted to. Considering the experimental set-up, with the nanotube oscillating parallel to the substrate, the conventional force curve cannot be easily acquired. However, it is in principle doable by following the position of the beam controller to keep the secondary electron emission constant. By approaching the substrate to the nanotube in a classical geometry a standard approach force curve could be therefore acquired. Together with the measurement of the conservative force gradient via the frequency shift and the dissipative forces via the change in the quality factor, this method allows to completely characterise the force environment with an unprecedented resolution.

Altogether our pioneering work demonstrates that one dimensional oscillators such as boron nitride nanotubes can be harnessed as probe sensors for Scanning Force Microscopy. By using a highly focused electron beam we can detect and record the mechanical response of an individual nanotube. Coupling atomic force microscopy technology together with high resolution electron beam detection, allows to measure, in real-time, conservative and dissipative interactions as well as the complete static interactions of a nanotube with its environment. We



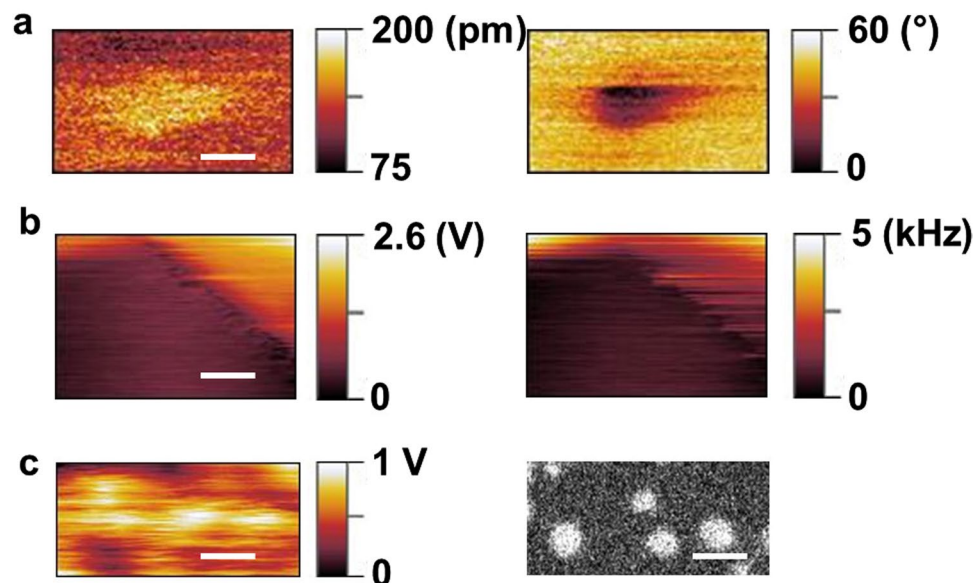


**Figure 3.** Nanotube-based Scanning Force Microscopy. (a) Amplitude (left) and phase (right) of the nanotube mechanical motion while scanning a sharp tungsten tip; the measurement reproduces correctly the force field induced by the tip and reconstructs the tip shape. Scale bar is 200 nm. (b) Scanning force imaging of a (100) silicon surface; the excitation amplitude keeping the nanotube oscillation amplitude constant (left) and the frequency shift (right) reproduce the surface topography of a 1  $\mu\text{m}$  terrace. Scale bar is 500 nm. (c) Static AFM image (left) and SEM picture (right) of gold nanoparticles deposited on a HOPG sample. The static AFM image is obtained by recording the deflection of the nanotube due to its interaction with the substrate; this quantity is given by the voltage command to the deflection coils which keeps constant the SE emission intensity. Scale bar is 500 nm.

elegantly exploited this new detection method to measure the surface topography of samples approached by the extremity of an individual nanotube.

In this first proof of concept of nanotube based atomic force microscope, we have performed measurements with a nanotube whose diameter and therefore apex is approximately 50 nm. As in standard atomic force, the spatial resolution is given by the probe apex and in this first work is in order of tens of nanometers. This limitation is only due to the choice of nanotube and thanks to the potentiality of the detection scheme, smaller nanotube can be used and even single wall nanotubes with diameters in the range of few nanometers<sup>20</sup>. Using single wall nanotubes will consequently decrease the spatial resolution at the level of cantilever functionalised with nanotube at the extremity. When using ultimate resonators, thermal noise will be a limiting factor to take into account; large thermally induced oscillation amplitude exceeding the diameter of nanotubes have been measured on individual carbon nanotube using electron beam detection<sup>20</sup> and this will be limiting the actual spatial resolution of a single wall nanotube based force microscopy. However we believe that thermal noise can be also turned to advantage allowing to develop a vectorial thermal noise-based force spectroscopy. In practice this would mean to extend what has been elegantly shown with Silicon Carbide nanowires<sup>10,19</sup> to individual nanotubes. This is however beyond the limit of this work. More in general, the highly focused electron beam allows to detect oscillators with diameters in the nanometer range, drastically increasing the force sensitivity and spatial resolution compared to standard atomic force microscope cantilevers and even more recent nanowires. Our work represents a proof of concept and open the path for the development of a new class of ultrasensitive nanotube-based scanning force microscopes.

## Methods

**Implementation.** Nanotubes are prepared by gluing them individually on an electrochemically etched tungsten tip. BNNTs are culled under optical observation and glued with carbon tape under optical microscope. On the sample holder of the Scanning Electron Microscope (NovaNanosem 450), the prepared nanotubes and the sample are placed face-to face on the same dedicated nanomanipulation station. The tip-nanotube is placed on a three axis steppers motors (3\*Smact SLC17-1720). The sample is placed on a three axis piezo-scanner with sub-nanometric resolution in displacement (MicroTRITOR Piezosystemjena). The nanotube and the sample are placed perpendicularly in the so-called pendulum configuration; i.e. the oscillations of the nanotube are parallel to the substrate. A piezo-dither (PA3JEW Thorlabs) is glued underneath the tip-nanotube to excite mechanically the nanotube at its natural frequency.

**Control in Real-Time.** During the experiments, measurements and controls are performed in Real-time by a complete Specs-Nanonis package (RT5, SC5 and OC4). The position of the electron beam of the SEM is controlled with the Specs-Nanonis electronics by directly controlling the voltage applied to the beam deflector lenses.

The secondary electrons emitted by the nanotubes are collected with a standard Everhart-Thornley Detector, which includes a strongly biased grid and a high bandwidth scintillator. The signal from the detector is then acquired and analysed via the Specs-Nanonis electronics.

## References

1. Niguès, A., Siria, A., Vincent, P., Poncharal, P. & Bocquet, L. Ultrahigh interlayer friction in multiwalled boron nitride nanotubes. *Nature materials* **7**, 688–693 (2014).
2. Ternes, M., Lutz, C. P., Hirjibehedin, C. F., Giessibl, F. J. & Heinrich, A. J. The Force Needed to Move an Atom on a Surface Measuring the Charge State of an Adatom with Noncontact Atomic Force Microscopy. *Science* **111**, 1066 (2008).
3. Socoliuc, A. *et al.* Atomic Scale control of Friction by actuation of nanometer-sized contacts. *Science* **207**, 207–210 (2006).
4. Kisiel, M. *et al.* Suppression of electronic friction on Nb films in the superconducting state. *Nature Materials* **2**, 119–122 (2011).
5. Binnig, J., Quate, C. F. & Gerber, C. Atomic force microscope. *Phys. Rev. Lett.* **56**, 930–934 (1986).
6. Giessibl, F. J. Atomic resolution of the silicon (111)-(7x7) surface by atomic force microscopy. *Science* **13**, 68–70 (1995).
7. Giessibl, F. J. Advances in atomic force microscopy. *Rev. Mod. Phys.* **3**, 949–983 (2003).
8. Barwich, V. *et al.* Carbon nanotubes as tips in non-contact SFM. *Applied Surface Science* **4**, 269–273 (2000).
9. Niguès, A., Siria, A., Verlot, P. Dynamical Backaction Cooling with Free Electrons, Nature Communications, doi:<https://doi.org/10.1038/ncomms9104> (2015).
10. Gloppe, A. *et al.* Bidimensional nano-optomechanics and topological backaction in a non-conservative radiation force field. *Nature Nanotechnology* **9**, 920–926 (2014).
11. Poncharal, P., Wang, Z., Ugarte, D. & de Heer, W. A. Electrostatic deflections and electromechanical resonances of carbon nanotubes. *Science* **283**, 1513–1516 (1999).
12. Moser, J., Eichler, A., Güttinger, J., Dykman, M. I. & Bachtold, A. Nanotube mechanical resonators with quality factors of up to 5 million. *Nature Nanotechnology* **12**, 1007–1011 (2014).
13. Steele, G. A., Strong Coupling Between Single-Electron Tunneling and Nanomechanical Motion, *Science*, 1103 (2011).
14. Lassagne, B., Tarakanov, Y., Kinaret, J., Garcia-Sanchez, D. & Bachtold, A. Coupling mechanics to charge transport in carbon nanotube mechanical resonators. *Science* **325**, 1107–1110 (2009).
15. Miao, T., Yeom, S., Wang, P., Standley, B. & Bockrath, M. Graphene nanoelectromechanical systems as stochastic-frequency oscillators. *Nano Letters* **6**, 2982–2987 (2014).
16. De Alba, R. *et al.* Tunable phonon cavity coupling in graphene membranes. *Nature Nanotechnology* **11**, 741–746 (2016).
17. Chaste, J. *et al.* A nanomechanical mass sensor with yoctogram resolution. *Nature Nanotechnology* **5**, 301–304 (2012).
18. de Lépinay, L. *et al.* A universal and ultrasensitive vectorial nanomechanical sensor for imaging 2D force fields. *Nature Nanotechnology* **12**, 156–162 (2016).
19. Rossi, N. *et al.* Vectorial scanning force microscopy using a nanowire sensor. *Nature Nanotechnology* **12**, 150–155 (2017).
20. Tsioutsios, I., Tavernarakis, A., Osmond, J., Verlot, P. & Bachtold, A. Real-time measurement of nanotube resonator fluctuations in an electron microscope. *Nano Letters* **17**, 1748–1755 (2017).
21. Bechelany, M. *et al.* Preparation of BN Microtubes / Nanotubes with a Unique Chemical Process. *The Journal of Physical Chemistry C* **47**, 18325–18330 (2008).
22. Kwon, S. *et al.* Experimental determination of the spring constant of an individual multiwalled carbon nanotube cantilever using fluorescence measurement. *Appl. Phys. Lett.* **95**, 013110–013112 (2009).
23. Karrai, K. & Grober, R. D. Piezoelectric tip-sample distance control for near field optical microscopes. *Appl. Phys. Lett.* **14**, 1842–1844 (1995).

## Acknowledgements

Authors acknowledge funding from the European Union's H2020 Framework Programme/ERC Starting Grant agreement number 637748 - NanoSOFT.

## Author Contributions

A.S. and A.N. contribute equally at this work.

## Additional Information

**Competing Interests:** The authors declare that they have no competing interests.

**Publisher's note:** Springer Nature remains neutral with regard to jurisdictional claims in published maps and institutional affiliations.



**Open Access** This article is licensed under a Creative Commons Attribution 4.0 International License, which permits use, sharing, adaptation, distribution and reproduction in any medium or format, as long as you give appropriate credit to the original author(s) and the source, provide a link to the Creative Commons license, and indicate if changes were made. The images or other third party material in this article are included in the article's Creative Commons license, unless indicated otherwise in a credit line to the material. If material is not included in the article's Creative Commons license and your intended use is not permitted by statutory regulation or exceeds the permitted use, you will need to obtain permission directly from the copyright holder. To view a copy of this license, visit <http://creativecommons.org/licenses/by/4.0/>.

© The Author(s) 2017